Proceedings of the Fifth International Conference on Communication and Electronics Systems (ICCES 2020)
IEEE Conference Record # 48766; IEEE Xplore ISBN: 978-1-7281-5371-1

Slantlet Radar Waveform for Effective Side-Lobe Suppression

Gnane Swarnadh Satapathi, Prakash karambally Shetty, Manjukiran Bagimane
Department of Electronics and Communication Engineering
AJ Institute of Engineering and Technology
Mangalore, Karnataka 575006
Email: gnaneswarnadhsatapathi@ajiet.edu.in

***Abstract*—In this paper, a cognitive radar waveform is proposed by using Slantlet filter coefficients. The construction of slantlet waveform is introduced and compared to conventional linear frequency modulated (LFM) with the same time duration and bandwidth. The results reveal that the proposed slantlet waveform has superior side-lobe suppression than the LFM signal. As the waveform is a combination of Slantlet filter coefficients, the amplitude and phase adjustment becomes flexible in various environments. Subsequently it can be used in cognitive radar.**

***Keywords*—auto-correlation, peak side lobe ratio, pulse compression radar, slantlet**

I. Introduction

Adaptive waveform plays an important role in cognitive radar for sensing the environment and decision making. Typically, the conventional radar waveform that is being used from a long time suffers from severe side-lobes. Because of these side-lobes, the ambiguity in range appears when the Doppler effect arises. The condition goes worse when the two targets are closely spaced.

Linear frequency modulation (LFM) waveform is traditionally used pulse compression waveform to detect both range and velocity [1]. But, the LFM suffers from significant side-lobes, which in turn minimizes the range resolution of the radar. Moreover, LFM has the frequency spread value and its not idle for detecting target velocity [2]. The Costas waveform [3] and stepped frequency modulated (SFM) [2] waveform degrades both the range resolution and Doppler as they have frequency spread term and high side-lobes. The phase coded waveform like Golay code [4], Barker code [5], Frank code [6] and $P1$, $P2$, Px codes [7] produces low/ zero side-lobes, but solemnly deteriorates as the Doppler effect occurs. Further, Prouhet-Thue-Morse (PTM) sequences are suggested to eliminate Doppler effect in a particular frequency limit [8]. However, the length of PTM sequences are very large and practically increases the complexity of the hardware. Moreover, many optimizing techniques have been proposed to reduce the side-lobe by reducing the amplitude of the main lobe [9]–[11].

In recent years, compressed sensing techniques are employed in radar for enhancing the range, velocity and spatial resolutions by suppressing the side-lobes [12]–[14]. But, more amount of time consumed to get L^1 norm solution and some times it might be unsolvable. A new waveform based on wavelet packets has been proposed to improve the range and Doppler resolution [15], [16]. To further suppress the side-lobes, traditional windowing technique is suggested in [17]. Morelet wavelet is suggested as adaptive waveform for MIMO radars [18].These wavelet based radar waveforms have been examined for wide variety of applications such as detection of moving targets [19], synthetic aperture radar (SAR) [20], adaptive radar [21] etc.

In this paper, we propose a new adaptive radar waveform based on slantlet filter banks. The slantlet filters are improved version of wavelet filters in terms of time localization and having good number of zero moments of the basis. The depiction of multi-resolution signals in both temporal and frequency domains permit the radar waveform design in either single or multiple sub-bands. The magnitude as well as phase of single or multiple sub-bands can be adjusted so as to improve the detection of the targets and this is the major need in adaptive waveform design. Further, the bandwidth in each sub-band is adjustable. The major focus in this paper is on constructing the waveform and improvement in peak side-lobe ratio value.

The anatomy of the paper is as follows. Section II describes about slantlet filter bank. The comparison of slantlet scaling function with LFM of same time interval and bandwidth is considered so as to convey the effective side-lobe suppression is presented in section III. The design of slantlet radar waveform and comparing with LFM is incorporated in section IV. Finally, the conclusion is discussed in section V.

II. Slantlet Filter Bank

The slantlet filter considered here is based on the secondary structure of discrete wavelet transform (DWT) which covers a user defined frequency range. The filters used here are dissimilar at each scale. These filters can produce high pulse compression rate with small side-lobe in its auto-correlation operation. Figure 1 depicts the filter structure and the derivation of filter coefficients as follows.

Let, m be the scale of filter bank, then the filter bank comprises of $2m$ channels and the length of the each filter is 2^m. Let, $a_m(n)$ and $b_m(n)$ are low pass filter and its adjacent filter coefficient respectively. The left over $2m-2$ channles have $c_i(n)$ filter coefficients with shifted time reverse for p=1,2,3,. . .,m-1. The filter coefficients of $c_m(n)$ are sampled by 2^{p+1}.

Let $a_m(n)$, $b_m(n)$ and $c_m(n)$ be piece-wise linear over the interval $n \in \{0, 1, 2, \ldots, 2^p - 1\}$ and $n \in \{2^p, 2^p +$

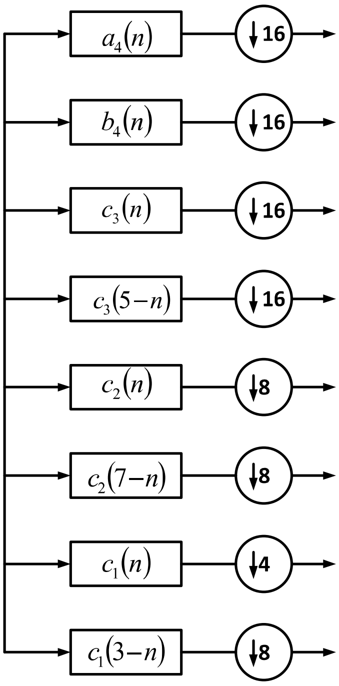

Fig. 1. Four-scale slantlet filter-bank

$1,\ldots,2^{p+1}-1\}$. In addition to it, $c_m(n)$ and $b_m(n)$ are considered to have two zero moments. Further, the functions $a_k(n)$, $b_k(n)$ and $c_k(n)$ are to be orthogonal to each other if $k > m$. The same is legitimate for the shifted versions of $c_m(n-2^m)$, $b_m(n-2^m)$ and their time reversed variants.

The filter $c_m(n)$ has to be linear over the intervals $n \in \{0,1,2,\ldots,2^p-1\}$ and $n \in \{2^p, 2^p+2, 2^p+2, \ldots, 2^{p+1}-1\}$ is expressed by using four parameters which is given in Equation 1 .

$$c_m(n) = \begin{cases} f_0 + f_1 n; & n = 0,1,2,\ldots,2^p-1 \\ f_2 + f_3(n-2^p); & n = 2^p, 2^p+1, \ldots, 2^{p+1}-1 \end{cases} \tag{1}$$

The values of f_0, f_1, f_2 and f_3 are to be computed in order to calculate the p scale orthogonal filter bank. Such that

1) $c_m(n)$ is of unit norm

$$\sum_{n=0}^{2^{p+1}-1} c_m^2(n) = 1 \tag{2}$$

2) $c_m(n)$ is orthogonal to its time reverse shifted versions

$$\sum_{n=0}^{2^{p+1}-1} c_m(n)c_m(2^{p+1}-1-n) = 0 \tag{3}$$

3) $c_m(n)$ extirpates linear discrete time polynomials

$$\sum_{n=0}^{2^{p+1}-1} c_m(n) = 0; \sum_{n=0}^{2^{p+1}-1} n c_m(n) = 0 \tag{4}$$

The above conditions can be rewritten by using the parameters (f_0, f_1, f_2 and f_3) so as to realize in terms of multivariate polynomial equations. By using the assistance of computer algebra [22] the expression of $c_m(n)$ is derived as

$$c_m(n) = \begin{cases} f_0 + f_1 n; & n = 0,1,2,\ldots,2^p-1 \\ f_2 + f_3(n-2^p); & n = 2^p, 2^p+1, \ldots, 2^{p+1}-1 \end{cases} \tag{5}$$

where,

$$\begin{aligned} q &= 2^p \\ h_1 &= 6\sqrt{q/((q^2-1)(4q^2-1))} \\ i_1 &= 2\sqrt{3/(q\cdot(q^2-1))} \\ h_0 &= -h_1\cdot(q-1)/2 \\ i_0 &= ((q+1)\cdot h_1/3 - q i_1)(q-1)/(2q) \\ f_0 &= (h_0+i_0)/2 \\ f_2 &= (h_0-i_0)/2 \\ f_1 &= (h_1+i_1)/2 \\ f_3 &= (h_1-i_1)/2. \end{aligned}$$

Similarly, by assuming the conditions of piecewise linear form, orthogonality and multivariate polynomial equations, the filter co-efficient of $a_m(n)$ and $b_m(n)$ are computed as

$$a_m(n) = \begin{cases} g_0 + g_1 n; & n = 0,1,2,\ldots,2^p-1 \\ g_2 + g_3(n-2^p); & n = 2^p, 2^p+1, \ldots, 2^{p+1}-1 \end{cases} \tag{6}$$

$$b_m(n) = \begin{cases} h_0 + h_1 n; & n = 0,1,2,\ldots,2^p-1 \\ h_2 + h_3(n-2^p); & n = 2^p, 2^p+1, \ldots, 2^{p+1}-1 \end{cases} \tag{7}$$

The orthogonality and moment conditions require the following

1) $a_m(n)$ and $b_m(n)$ are of unit norm

$$\sum_{n=0}^{2^{p+1}-1} a_m^2(n) = 1 \quad \text{and} \quad \sum_{n=0}^{2^{p+1}-1} b_m^2(n) = 1 \tag{8}$$

2) $a_m(n)$ and $b_m(n)$ are orthogonal to their time reversed shifted versions

$$\sum_{n=0}^{2^p-1} a_m(n)a_m(n+2^P) = 0 \tag{9}$$

$$\sum_{n=0}^{2^p-1} b_m(n)b_m(n+2^P) = 0 \tag{10}$$

$$\sum_{n=0}^{2^{p+1}-1} a_m(n)b_m(n) = 0 \tag{11}$$

$$\sum_{n=0}^{2^p-1} a_m(n)b_m(n+2^P) = 0 \tag{12}$$

3) $a_m(n)$ and $b_m(n)$ expatriates as linear discrete time polynomials

Proceedings of the Fifth International Conference on Communication and Electronics Systems (ICCES 2020)
IEEE Conference Record # 48766; IEEE Xplore ISBN: 978-1-7281-5371-1

$$\sum_{n=0}^{2^{p+1}-1} a_m(n) = 0 \tag{13}$$

$$\sum_{n=0}^{2^{p+1}-1} n a_m(n) = 0 \tag{14}$$

$$\sum_{n=0}^{2^{p+1}-1} b_m(n) = 0 \tag{15}$$

$$\sum_{n=0}^{2^{p+1}-1} n b_m(n) = 0 \tag{16}$$

where,

$$\begin{aligned}
q &= 2^p \\
u_1 &= 1/\sqrt{q} \\
u_2 &= \sqrt{(2q^2+1)/3} \\
g_0 &= u_1(u_2+1)/(2q) \\
g_2 &= u_1(2q-u_2-1)/(2q) \\
g_1 &= u1/q \\
g_3 &= -g_1 \\
u_3 &= \sqrt{3/(q \cdot (q^2-1))/q} \\
h_1 &= u_3(u_2-q) \\
h_3 &= -u_3 \cdot (u_2+q) \\
h_2 &= h_3 \cdot (u_2+1-2q)/2 \\
h_0 &= h_1 \cdot (u_2+1)/2
\end{aligned}$$

The signs of the square roots in filter coefficients $(a_m(n)), b_m(n) and c_m(n)$ can be reversed. Doing so, simply negates or time reverses the sequence. A brief description about slantlet filter is given in [23]. As the integer translates of filter coefficients are orthogonal to each other, then

$$\sum l(n)l(n-2k) = \delta(k) \quad \text{where} \quad l = g, h, f \tag{17}$$

The discrete auto-correlation of slantlet filter coefficients is a delta function, which is perfect for radar signal. Since, the delta function does not have any side-lobes, closely spaced targets will not interfere each other. Therefore, slantlet filter coefficients has the potential to generate high resolution radar compressed signals.

III. Comparison of LFM with Slantlet Scaling-4 Coefficients

The linear frequency modulated (LFM) waveform is being used as a conventional waveform from a long time. The equation for LFM waveform is given as

$$x(t) = sin\left[(f_c + \beta t) + \phi\right] \tag{18}$$

where, f_c, β. ϕ are carrier frequency, modulation rate and phase angle respectively. The values of f_c, t and β are considered as 0Hz, 3sec, and 0.59 rad/sec, so that we can compare the LFM with slantlet waveform. The parameters are considered in such a way that both the waveforms have same time span and 3dB bandwidth.

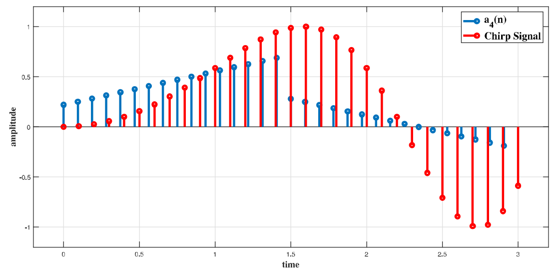

Fig. 2. The $a_4(n)$ filter coefficient and LFM Signal

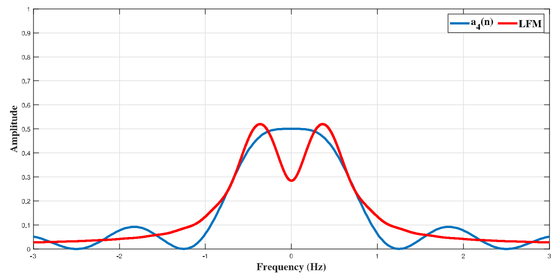

Fig. 3. The Spectrum of $a_4(n)$ filter coefficient and LFM Signal

Figure 2 depicts the low rate LFM signal and $a_4(n)$ signal with 3sec time duration. Whereas, the spectrum of $a_4(n)$ and LFM of 3 sec time duration are shown in Figure 3. The auto-correlations of both LFM and $a_4(n)$ waveforms are illustrated in Figure 4. The LFM waveform has a narrower main-lobe when compared to $a_4(n)$. But, $a_4(n)$ has almost zero side-lobes in contrast with LFM. This criterion is very important in ideal radar so as to enhance the radar range resolution and also to classify between closely spaced targets.

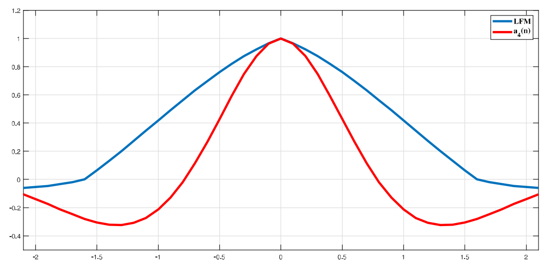

Fig. 4. Autocorrelations of $a_4(n)$ and LFM Signal

The different spectrum of two different waveforms can also provide some information about the auto-correlation. Due to the time frequency duality nature, the rectangular waveform has a sinc spectrum and vice-versa. Therefore, if the aim of auto-correlation is rectangle like function, then the spectrum should be sinc. Figure 4 portray that, $a_4(n)$ has sinc spectrum, while LFM has decaying spectrum and vice versa in temporal domain (See Figure 3).

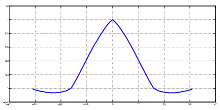

(a) Autocorrelation of $a_4(n)$

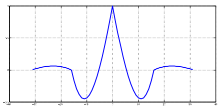

(b) Autocorrelation of $b_4(n)$

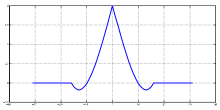

(c) Sum of Autocorrelation of $a_4(n)$ and $b_4(n)$

Fig. 5. Sum of Autocorrelation of $a_4(n)$ and $b_4(n)$ to get a compressed signal

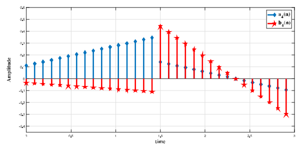

(a) 6.a

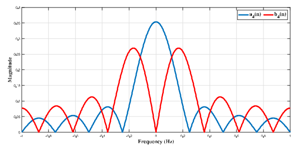

(b) 6.b

Fig. 6. $a_4(n)$ (blue) and $b_4(n)$ (red) in time domain (6.a) and the frequency domain (6.b)

IV. Proposed Waveform by Using Slantlet Filter Coefficients

A. Sum of auto-correlation of Slantlet filter coefficients

The new radar waveform is designed by combining the scaling functions of slantlet waveform. The slantlet filter bank is considered as secondary structure of wavelet [23]. Moreover, slantlet is an exceptional case which depends on Gram-Schmidt orthogonality. The slantlet filter coefficients are orthogonal, piece-wise linear with two zero moments and has octave band characteristic. Besides that slantlet filter bank provides a scale decomposition factor of 2 and has a multi resolution decomposition. Even though slanlet does not have a tree structure, it can be implemented accurately similar to iterated discrete wavelet filter bank [16].

Figure 5 portray auto-correlation of $a_4(n)$, $b_4(n)$ and sum of both. The resultant compressed waveform has half the duration of $a_4(n)$. The compressed auto-correlation can be explained better with spectrum of $a_4(n)$ and $b_4(n)$. It can be clearly observed from Figure 6 that the spectrum of $a_4(n)$ and $b_4(n)$ are complimented to each other. So, the resultant auto-correlation is compressed by duration of half.

If one filter coefficient if slantlet is embedded into a pulsed waveform with pulse width of $1\mu sec$ then the resultant bandwidth will be $3MHz$. Furthermore if eight slantlet filter coefficients are embedded in the same $1\mu sec$ pulse width then the bandwidth can raise up to 192 MHz. All individual eight slantlet filter coefficients are plotted in Figure 8. Their individual auto-correlations and sum of all auto-correlation is illustrated in Figure 9. It can also be observed that all the eight auto-correlation values are not similar and resultant value is approximately equal to delta function. In the next subsection, slantlet radar waveform is discussed which attains high side-

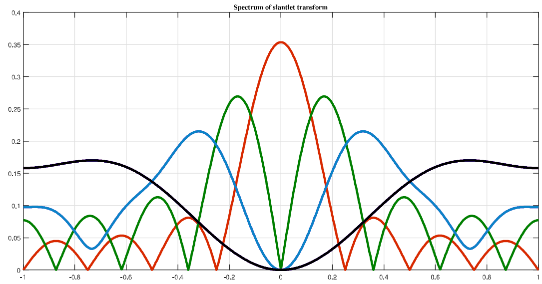

Fig. 7. Spectrum of Slantlet filter coefficients

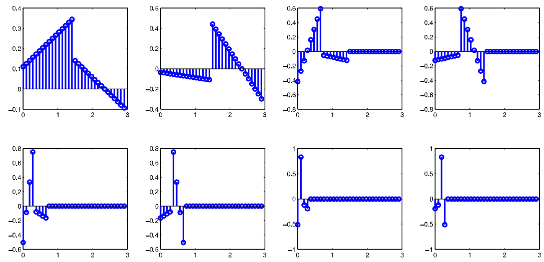

Fig. 8. The waveforms of the individual Slantlet Filter coefficients

lobe suppression level. Further this new waveform can be used in cognitive radar in future.

B. Comparison of Slantlet radar waveform with conventional LFM

The proposed waveform is generated by concatenating the slantlet filter coefficients, such that the auto-correlation of the waveform has almost zero side-lobes. The slantlet waveform is compared with LFM waveform with same bandwidth. Figure 10 depicts the time-frequency diagram of LFM and slanlet waveforms. It can be clearly observed from Figure 10 that, the frequency is varying linearly and discretely for LFM and slantlet waveform respectively. Moreover, the frequency is varying with Δt, time duration for slantlet waveform. The frequency cannot be determined in Δt as the sub-bands of each slantlet filter is placed in the time interval. In slantlet filter, both the parameters phase and amplitude can be varied on a specific filter coefficient.

TABLE I. Comparison of PSLR for different waveforms

Sl No	Waveform	Peak side lobe ratio (in dB)
1	LFM	13.2
2	Wavelet	20.6
3	Slantlet	21.15

The filter coefficients of slantlet filter banks are concatenated to produce a new radar waveform as shown in Figure 11. The auto-correlation of slantlet waveform and LFM is carried out in continuous domain rather than discrete domain. One can observe clearly that the auto-correlation of slantlet waveform has almost no side-lobes (see Figure 12). Where as the auto-correlation of LFM has one side-lobe on each side

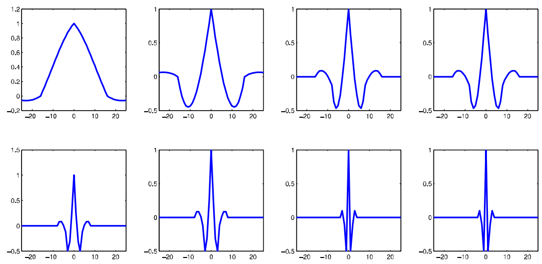

(a)

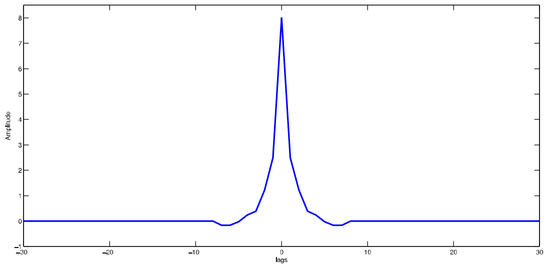

(b)

Fig. 9. Autocorrelation of the 8 Slantlet filter coefficients (Figure 9.a) and Summation of the 8 autocorrelations (Figure 9.b)

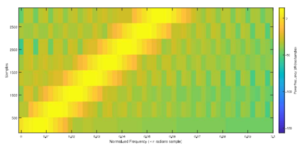

(a) 10.a

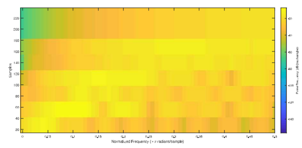

(b) 10.b

Fig. 10. Spectrogram of LFM in Figure 10.a and slantlet in Figure 10.b respectively

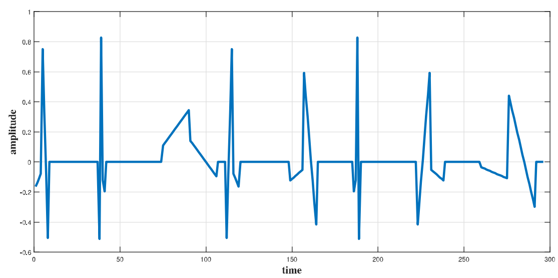

Fig. 11. Slantlet radar waveform

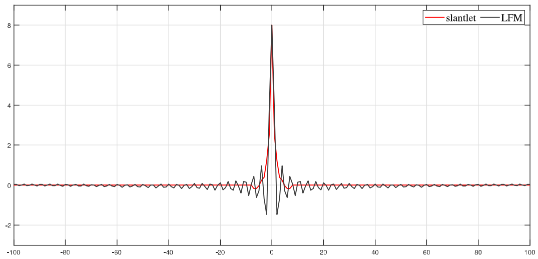

Fig. 12. Comparison of auto-correlation between LFM and slantlet radar waveform

of main lobe. The peak to side lobe ratio (PSLR) of slantlet waveform is 21.15dB when compared to 13.2dB of the LFM. Table I shows the comparison of PSLR of slantlet waveform with earlier proposed techniques. Moreover the bandwidths of each filter need not be constant. Both the filter length and bandwidth can be varied by using the technique in [16]. So, as per different environmental conditions and applications one can vary the bandwidth and length of filter coefficient.

Therefore, from the above results, the slantlet waveform can suppress the side-lobe more effectively when compared to LFM. Moreover, the spectrum and length of each filter coefficient can be changed which in turn are the characteristics of adaptive radar waveform.

V. Conclusion

In this paper, a new radar waveform based on slantlet filter bank is proposed. The auto correlation of the proposed waveform is a delta function and each filter bank is orthogonal with other filter banks. Further, one can choose a specific filter bandwidth in order to generate corresponding radar waveform. Additionally, the proposed waveform can be adapted to the environment by varying magnitude and phase of a particular frequency band. Results show that there is a significant suppression in side-lobe when compared to LFM and wavelet waveforms. Due to above mentioned advantages, slantlet waveform can be used in cognitive radar. Automatic selection of filter banks according to the environment will be studied in future,

References

[1] D. Sidney, “Pulse transmission,” May 18 1954, uS Patent 2,678,997.

[2] G. Gill, “Simultaneous pulse compression and doppler processing with step frequency waveform,” *Electronics letters*, vol. 32, no. 23, pp. 2178–2179, 1996.

[3] J. P. Costas, “A study of a class of detection waveforms having nearly ideal range—doppler ambiguity properties,” *Proceedings of the IEEE*, vol. 72, no. 8, pp. 996–1009, 1984.

[4] A. Pezeshki, A. R. Calderbank, W. Moran, and S. D. Howard, “Doppler resilient golay complementary waveforms,” *IEEE Transactions on Information Theory*, vol. 54, no. 9, pp. 4254–4266, 2008.

[5] R. Barker, “Group synchronizing of binary digital sequences,” *Communication Theory*, 1953.

[6] R. Frank, “Polyphase codes with good nonperiodic correlation properties,” *IEEE Transactions on Information Theory*, vol. 9, no. 1, pp. 43–45, 1963.

[7] B. L. Lewis and F. F. Kretschmer, "Linear frequency modulation derived polyphase pulse compression codes," *IEEE Transactions on Aerospace and Electronic Systems*, no. 5, pp. 637–641, 1982.

[8] Y. Chi, A. Pezeshki, R. Calderbank, and S. Howard, "Range sidelobe suppression in a desired doppler interval," in *2009 International Waveform Diversity and Design Conference*. IEEE, 2009, pp. 258–262.

[9] H. C. Stankwitz, R. J. Dallaire, and J. R. Fienup, "Nonlinear apodization for sidelobe control in sar imagery," *IEEE Transactions on Aerospace and Electronic Systems*, vol. 31, no. 1, pp. 267–279, 1995.

[10] C. H. Seo and J. T. Yen, "Sidelobe suppression in ultrasound imaging using dual apodization with cross-correlation," *IEEE transactions on ultrasonics, ferroelectrics, and frequency control*, vol. 55, no. 10, pp. 2198–2210, 2008.

[11] L. R. Varshney and D. Thomas, "Sidelobe reduction for matched filter range processing," in *Proceedings of the 2003 IEEE Radar Conference (Cat. No. 03CH37474)*. IEEE, 2003, pp. 446–451.

[12] M. Herman and T. Strohmer, "Compressed sensing radar," in *2008 IEEE Radar Conference*. IEEE, 2008, pp. 1–6.

[13] C.-Y. Chen and P. Vaidyanathan, "Compressed sensing in mimo radar," in *2008 42nd Asilomar Conference on Signals, Systems and Computers*. IEEE, 2008, pp. 41–44.

[14] L. C. Potter, E. Ertin, J. T. Parker, and M. Cetin, "Sparsity and compressed sensing in radar imaging," *Proceedings of the IEEE*, vol. 98, no. 6, pp. 1006–1020, 2010.

[15] S. Cao, Y. F. Zheng, and R. L. Ewing, "Scaling function waveform for effective side-lobe suppression in radar signal," in *Proceedings of the 2011 IEEE National Aerospace and Electronics Conference (NAECON)*. IEEE, 2011, pp. 231–236.

[16] ——, "A wavelet-packet-based radar waveform for high resolution in range and velocity detection," *IEEE Transactions on Geoscience and Remote Sensing*, vol. 53, no. 1, pp. 229–243, 2014.

[17] F. J. Harris, "On the use of windows for harmonic analysis with the discrete fourier transform," *Proceedings of the IEEE*, vol. 66, no. 1, pp. 51–83, 1978.

[18] C. Ji, Y. Song, and Q. Du, "Adaptive waveform design based on morlet wavelet for ultra-wideband mimo radar," *Journal of Systems Engineering and Electronics*, vol. 27, no. 2, pp. 362–369, 2016.

[19] S. Cao, Y. F. Zheng, and R. L. Ewing, "Wavelet-based radar waveform for moving targets detection," in *2014 IEEE Radar Conference*. IEEE, 2014, pp. 1149–1154.

[20] ——, "Wavelet-based gaussian waveform for spotlight synthetic aperture radar," in *NAECON 2014-IEEE National Aerospace and Electronics Conference*. IEEE, 2014, pp. 267–273.

[21] ——, "Wavelet-based radar waveform adaptable for different operation conditions," in *2013 European Radar Conference*. IEEE, 2013, pp. 149–152.

[22] G. Greuel, G. Pfister, and H. Schonemann, "Singular reference manual, reports on computer algebra, no. 12, centre of algebra, university of kaiserslautern, germany."

[23] I. W. Selesnick, "The slantlet transform," *IEEE transactions on signal processing*, vol. 47, no. 5, pp. 1304–1313, 1999.